Mendeleev Communications

Mendeleev Commun., 2025, **35**, 692–695

Structural descriptors for detecting order–disorder phase transitions in two-dimensional hybrid lead halide perovskites

Ekaterina I. Marchenko,*[a,b] Nikolay A. Belich,[a] Natalia N. Udalova,[a] Alexander S. Sudakov,[a] Nikolay N. Eremin,[b] Eugene A. Goodilin[a,c] and Alexey B. Tarasov[a,c]

[a] *Department of Materials Science, M. V. Lomonosov Moscow State University, 119991 Moscow, Russian Federation. E-mail: marchenko-ekaterina@bk.ru*
[b] *Department of Geology, M. V. Lomonosov Moscow State University, 119991 Moscow, Russian Federation*
[c] *Department of Chemistry, M. V. Lomonosov Moscow State University, 119991 Moscow, Russian Federation*

DOI: 10.71267/mencom.7823

Correlation analysis of geometric crystal chemical descriptors of the crystal structures of two-dimensional (2D) hybrid lead halide perovskite polymorphs revealed a strong correlation of the order–disorder phase transitions in these compounds with three geometric parameters, namely, the effective volume of the organic cation, the relative distance from the center of mass (RDCM) for the organic spacer cation in the cuboctahedral void of the layer of corner-shared octahedra and the equatorial M–X bond length. The calculated values of the band gaps for the order–disorder phase transitions in the investigated compounds vary up to 0.26 eV. These results will be useful in developing new design principles for tuning the physical properties *via* structural phase transitions in 2D hybrid lead halide perovskites.

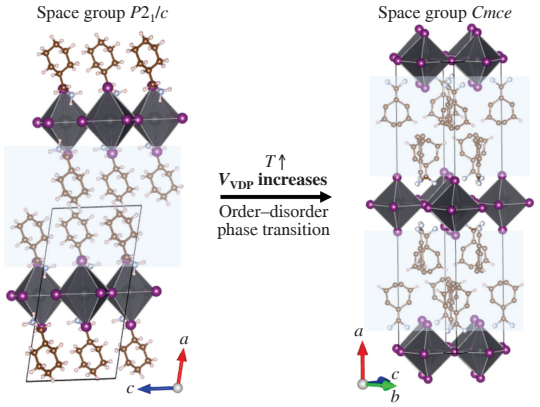

Keywords: hybrid perovskites, polymorphs, order–disorder phase transitions, two-dimensional structures, symmetry reduction, band gap.

Two-dimensional (2D) hybrid organic–inorganic halide perovskites (HOIPs) are a class of 2D semiconductors with high potential for applications in optoelectronics, spintronics and ferroelectrics. Their significant appeal for the fabrication of homojunctions arises from their tunable composition and structural phases, which provide a wide range of physical properties.[1–4] 2D HOIPs are characterized by a multi-quantum-well architecture comprising alternating organic and inorganic or hybrid layers, referred to as quasi-3D slabs. This unique structure can be synthesized by modulating the ratio of A-site cations to bulky spacer cations. The general formula for these materials can be expressed as $(A')_m(A)_{n-1}M_nX_{3n+1}$, where A′ denotes a large organic cation, A signifies a small organic cation (*e.g.*, methylammonium or formamidinium), M represents a divalent metal, and X indicates a halide. The parameters *m* and *n* correspond to the specific cation types and the quantum well thickness of the quasi-3D perovskite slabs, respectively. To date, more than 800 HOIP crystal structures with more than 250 different organic cations have been experimentally refined.[5]

Unlike conventional inorganic 2D materials such as graphene, MoS_2 and black phosphorus, which typically consist of a single inorganic layer or a few atomic layers, 2D HOIPs are distinguished by their organic–inorganic hybrid structures. The characteristic feature of these structures is intercalated organic spacers that are periodically interdigitated with inorganic metal halide slabs in a stacked arrangement. The selection of the organic cation allows for the control and tuning of local physical properties and facilitates the engineering of quantum confinement effects. The substantial size of the organic cations in the A′ site introduces excess strain, which often leads to octahedral distortions, thereby affecting the band gap and other optoelectronic characteristics of the materials.[6,7] One way to tune the optoelectronic properties of 2D perovskites is to control reversible polymorphic phase transitions[8–10] at different temperatures, at which the structure is rearranged and the packing of organic cation layers and geometric distortions in the inorganic substructure are changed.

In this work, based on the previously refined experimental structure, we show by crystal chemical analysis and theoretical calculations that 2D HOIPs with different organic spacer cations often undergo a solid–solid phase transition with temperature, during which the organic cations undergo an order–disorder transition with a change in the band gap. We identify structural descriptors that can be used to detect order–disorder phase transitions in 2D HOIPs.

A set of 20 crystal structures with Pb–I and Pb–Br inorganic substructures from the layered hybrid perovskite database[5] was used for the analysis. The structures refined at different temperatures represent polymorphs with 10 different organic spacer cations, namely undecylammonium **1**, tridecylammonium **2**, (cyclohexylmethyl)ammonium **3**, isobutylammonium **4**, [2-(4-bromophenyl)ethyl]ammonium **5**, pentylammonium **6**, (4,4-difluorocyclohexyl)ammonium **7**, hexylammonium **8**,

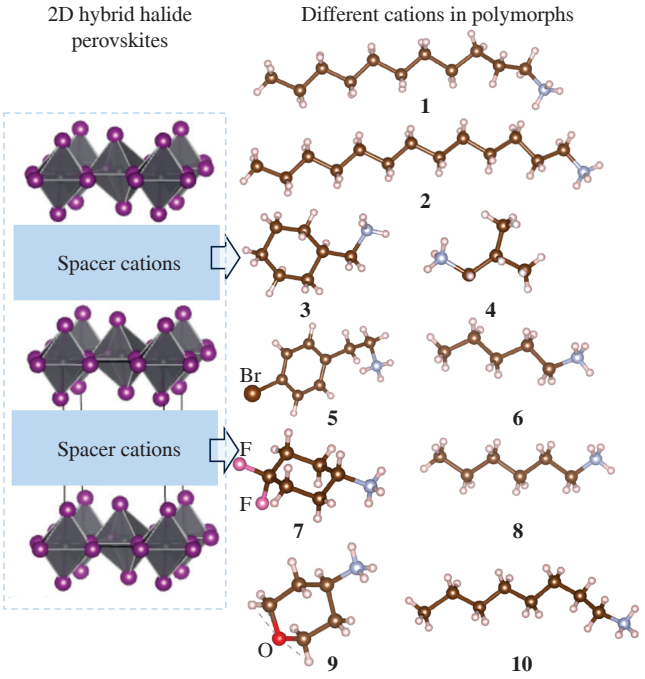

Figure 1 Ball-and-stick representation of various spacer cations located between inorganic layers in 2D perovskite polymorphs. Pb, I, C, N and H atoms are represented by grey, purple, brown, blue and pink spheres, respectively.

(tetrahydropyran-4-yl)ammonium **9** and octylammonium **10** (Figure 1).

For the structures under study (Table 1), the band gap values were calculated using the density functional theory (DFT) method.† The crystal structures of most high-temperature polymorphs (except for those with cations **2** and **9**) have orthorhombic space groups of higher symmetry compared to the low-temperature polymorphs crystallizing in the monoclinic system. It is expected that the more highly symmetric structures of compounds of this class will exhibit fewer distortions of the inorganic substructure, as a result of which the band gap will decrease.[6] However, the calculated band gap values do not always follow this trend. The band gap values for different polymorphs can be either virtually identical or differ significantly, reaching differences of up to 0.26 eV (as was observed in the case of 2D perovskites containing cations **5**). It is important to note that there is no clear trend in increasing or decreasing the band gap depending on the symmetry or crystallization temperature of the polymorphs. To clarify the reasons for this, we carried out a detailed crystal chemical analysis of the geometry of these structures.

By performing crystal chemical analysis of the polymorphs, we calculated such parameters of inorganic and organic substructures as axial and equatorial M–X bond lengths in octahedra, X–M–X bond angles in the plane and out of the plane

† The theoretical calculations of the band gap were performed using the Quantum Espresso package.[21] A plane-wave basis set was used together with the Perdew–Burke–Ernzerhof (PBE) exchange–correlation functional. The initial unit cell configurations for the 2D perovskites in this work were based on experimental X-ray diffraction data, the unit cell vectors and atom coordinates were optimized to have a force below 0.04 Ry (a.u.)$^{-1}$. The reciprocal space was sampled using 2×4×4 Monkhorst–Pack grids. The electrons of lead ($5d^{10}/6s^2/6p^2$), nitrogen ($2s^2/2p^3$), iodine ($5s^2/5p^5$) and carbon ($2s^2/2p^2$) were considered as valence electrons. The first included the PBE functional in the generalized gradient approximation using Vanderbilt-type, scalar relativistic pseudopotentials without spin–orbit coupling. VESTA software[22] was used to visualize crystal structures and organic cations.

Table 1 DFT-calculated band gap values for 2D hybrid perovskite polymorphs with different cations and space groups stable at different temperatures.

Cation A′	Perovskite formula	Calculated band gap/eV	*T*/K	Space group reported	Reference
1	$(A')_2PbI_4$	2.39	223	$P2_12_12_1$	11
		2.33	298	*Pbca*	11
2	$(A')_2PbI_4$	2.4	250	$P2_12_12_1$	11
		2.45	298	$P2_1/c$	11
3	$(A')_2PbI_4$	2.31	300	$P2_1/c$	12
		2.15	365	*Cmca*	12
4	$(A')_2PbBr_4$	2.83	293	$P2_1/c$	13
		2.84	393	*Cmca*	13
5	$(A')_2PbI_4$	2.31	100	*C*2/*c*	14
		2.05	295	*Cmca*	15
6	$(A')_2PbI_4$	2.37	173	$P2_1/a$	16
		2.29	333	*Pbca*	16
7	$(A')_2PbI_4$	2.38	293	$Cmc2_1$	17
		2.29	398	*Pbca*	17
8	$(A')_2PbI_4$	2.28	173	$P2_1/a$	16
		2.29	293	*Pbca*	16
9	$(A')_2PbBr_4$	2.83	293	$Cmc2_1$	18
		2.88	350	*P*1	19
10	$(A')_2PbI_4$	2.38	173	$P2_1/a$	20
		2.28	293	*Pbca*	20

of the inorganic substructure, M–X–M bond angles and RDCM values for organic spacer cations in cuboctahedral voids of the layer of corner-shared octahedra,‡,[23] as well as interlayer distances and effective volumes of organic spacer cations in the structures. The effective average volume of organic spacer cations (V_{VDP}) was calculated using the Voronoi–Dirichlet polyhedron construction‡ using the ToposPro software package.[24]

We then examined the differences in the values of all calculated geometric descriptors between the high- and low-temperature polymorphs containing the same organic cations and constructed a Pearson correlation matrix to identify the relationships between the geometric descriptors (Figure 2). The heat map of the Pearson correlation coefficients clearly illustrates that the correlation coefficients between V_{VDP} and the RDCM descriptor and the equatorial M–X distances are positive (0.87 and 0.78, respectively). Interestingly, no significant correlations were found between the other geometric descriptors for the studied polymorphs. In addition to the V_{VDP} analysis, we calculated the effective volumes (V_H) of the cations using the Hirschfeld isosurface method implemented in the Crystal Explorer software.[25] As expected, the calculated V_{VDP} and V_H values for organic cations in the structures correlate with each other (correlation coefficient 0.98), indicating the suitability of both methods for estimating cation sizes.

Thus, based on the correlation analysis, we have found that such geometric descriptors as the effective volume of the organic cation, RDCM and the equatorial M–X bond lengths (along the inorganic layers in the structures) in the MX_6 octahedra are the most significant geometric descriptors in polymorphic phase transitions in 2D hybrid perovskites.

‡ RDCM is defined as the distance between the center of positive charge of an organic cation and the center of mass of a void in an inorganic framework. The Voronoi–Dirichlet polyhedron (VDP) model of an atom in a crystal field adequately reflects the shape of an atomic domain. It allows crystal chemical analysis and can be used for a universal model of representing the crystal structure at the level of its geometric description. According to the definition of VDP, each VDP face divides the crystal space into two equal half-spaces belonging to one of the atoms separated by the face. The main algorithms for constructing VDPs are implemented in the ToposPro software package. VDP can often characterize not only the relative but also the absolute size of an atom in a crystal structure.

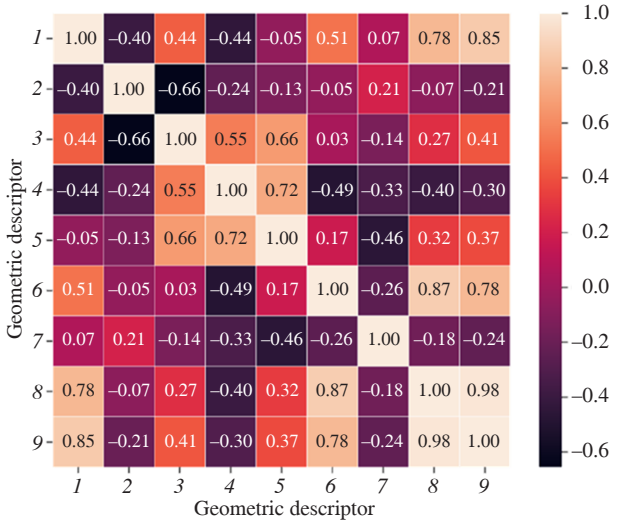

Figure 2 Heat map of the Pearson correlation coefficient matrix for geometric descriptors of 2D hybrid perovskite polymorphs: (*1*) equatorial M–X distance, (*2*) axial M–X distance, (*3*) in-plane X–M–X angle, (*4*) out-of-plane X–M–X angle, (*5*) M–X–M angle, (*6*) RDCM, (*7*) interlayer distance, (*8*) V_{VDP} and (*9*) V_H.

Polymorphic phase transitions in 2D HOIPs are classified as order–disorder transitions in organic cation layers, while the symmetry of the inorganic substructure in the disordered phase is often higher than in the ordered one [Figure 3(*a*)]. We believe that this fact is related to the peculiarities of the structural refinement of these disordered 2D HOIPs, so the presence of cationic disorder in these phases does not allow us to identify a clear relationship between the type of organic cation and the distortions of the inorganic substructure and, consequently, the band gap.

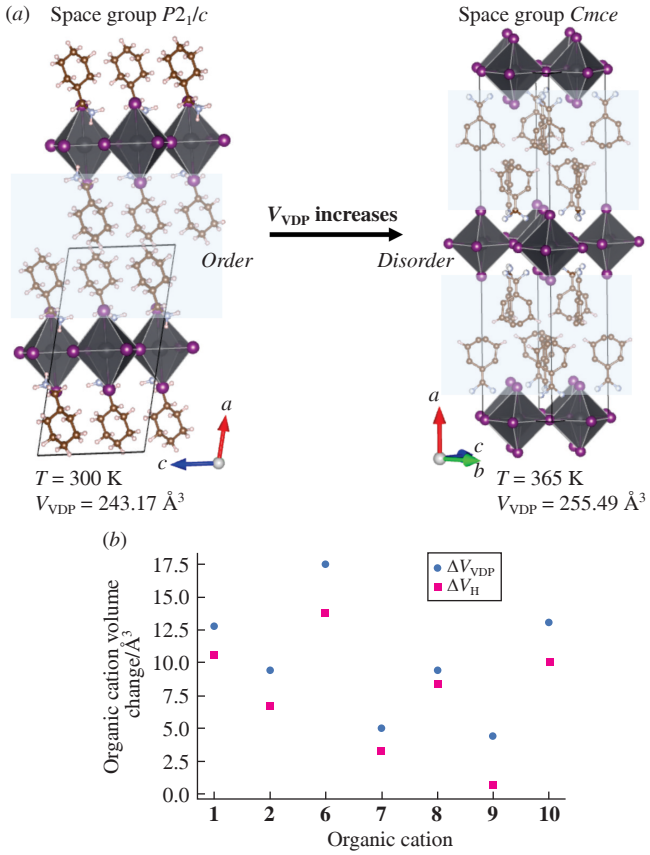

Figure 3 (*a*) 2D HOIP polymorphs with spacer cations **3** showing different topology of organic layers at different temperatures. (*b*) Difference in the calculated effective volume of the organic spacer cation between high- and low-temperature 2D HOIP polymophs calculated using the Voronoi–Dirichlet polyhedron and Hirshfield isosurface approaches.

It should be noted that the Voronoi–Dirichlet method overestimates the effective volume of cations compared to calculations using the Hirshfeld isosurface method [Figure 3(*b*)]. However, for most 2D HOIP structures, there is a tendency for the average volumes of organic cations in high-temperature polymorphs to increase compared to low-temperature ones, with the change in volume varying from 5 to 17.5 Å^3.

In summary, we have shown that three geometric descriptors are significant for detecting order–disorder phase transitions in twenty 2D HOIP polymorphs with various organic spacer cations crystallized at different temperatures, namely, the effective volume of the organic cation, RDCM for organic spacer cations in the cuboctahedral voids of the layer of corner-shared octahedra and the equatorial M–X bond length. In high-temperature polymorphs, the symmetry of the inorganic substructure is often higher than in low-temperature ones, while the atoms of the organic substructure are disordered. The difference in the calculated values of the band gap for polymorphs undergoing the order–disorder phase transition varies within 0.26 eV, but have no clear relationship with individual structural descriptors. These results expand our understanding of the various structural motifs of 2D HOIPs and clarify the impact of structural modifications on their properties, as well as open up opportunities for the design of solar cells, photodetectors and LEDs.

This work was supported by the Russian Science Foundation (grant no. 23-73-01212).

References

1 J.-C. Blancon, J. Even, C. C. Stoumpos, M. G. Kanatzidis and A. D. Mohite, *Nat. Nanotechnol.*, 2020, **15**, 969; https://doi.org/10.1038/s41565-020-00811-1.
2 J. Duan, J. Li, G. Divitini, D. Cortecchia, F. Yuan, J. You, S. (F.) Liu, A. Petrozza, Z. Wu and J. Xi, *Adv. Mater.*, 2024, **36**, 2403455; https://doi.org/10.1002/adma.202403455.
3 L. Mao, C. C. Stoumpos and M. G. Kanatzidis, *J. Am. Chem. Soc.*, 2019, **141**, 1171; https://doi.org/10.1021/jacs.8b10851.
4 Y. Gao, E. Shi, S. Deng, S. B. Shiring, J. M. Snaider, C. Liang, B. Yuan, R. Song, S. M. Janke, A. Liebman-Peláez, P. Yoo, M. Zeller, B. W. Boudouris, P. Liao, C. Zhu, V. Blum, Y. Yu, B. M. Savoie, L. Huang and L. Dou, *Nat. Chem.*, 2019, **11**, 1151; https://doi.org/10.1038/s41557-019-0354-2.
5 E. I. Marchenko, S. A. Fateev, A. A. Petrov, V. V. Korolev, A. Mitrofanov, A. V. Petrov, E. A. Goodilin and A. B. Tarasov, *Chem. Mater.*, 2020, **32**, 7383; https://doi.org/10.1021/acs.chemmater.0c02290.
6 E. I. Marchenko, V. V. Korolev, S. A. Fateev, A. Mitrofanov, N. N. Eremin, E. A. Goodilin and A. B. Tarasov, *Chem. Mater.*, 2021, **33**, 7518; https://doi.org/10.1021/acs.chemmater.1c02467.
7 E. I. Marchenko, V. V. Korolev, A. Mitrofanov, S. A. Fateev, E. A. Goodilin and A. B. Tarasov, *Chem. Mater.*, 2021, **33**, 1213; https://doi.org/10.1021/acs.chemmater.0c03935.
8 X.-N. Li, P.-F. Li, Z.-X. Wang, P.-P. Shi, Y.-Y. Tang and H.-Y. Ye, *Polyhedron*, 2017, **129**, 92; https://doi.org/10.1016/j.poly.2017.03.025.
9 E. J. Dalley, L. C. Bloxham, J. R. Muralidhar, P. W. Martin, I. J. Kim and C. G. Bischak, *ACS Energy Lett.*, 2024, **9**, 5756; https://doi.org/10.1021/acsenergylett.4c02645.
10 A. Singh, D. Dayton, D. M. Ladd, G. Reuveni, P. Paluch, L. Montagne, J. Mars, O. Yaffe, M. Toney, G. N. M. Reddy and D. B. Mitzi, *J. Am. Chem. Soc.*, 2024, **146**, 25656; https://doi.org/10.1021/jacs.4c07411.
11 A. Lemmerer, *Inorg. Chem.*, 2022, **61**, 6353; https://doi.org/10.1021/acs.inorgchem.1c03132.
12 Q.-Q. Jia, L. Tong, M.-M. Lun, D.-W. Fu, T. Zhang and H.-F. Lu, *Cryst. Growth Des.*, 2022, **22**, 2799; https://doi.org/10.1021/acs.cgd.2c00183.
13 Z.-X. Wang, W.-Q. Liao, H.-Y. Ye and Y. Zhang, *Dalton Trans.*, 2015, **44**, 20406; https://doi.org/10.1039/C5DT03277F.
14 D. B. Straus, N. Iotov, M. R. Gau, Q. Zhao, P. J. Carroll and C. R. Kagan, *J. Phys. Chem. Lett.*, 2019, **10**, 1198; https://doi.org/10.1021/acs.jpclett.9b00247.
15 H. Pan, X. Zhao, X. Gong, Y. Shen and M. Wang, *J. Phys. Chem. Lett.*, 2019, **10**, 1813; https://doi.org/10.1021/acs.jpclett.9b00479.

16 D. G. Billing and A. Lemmerer, *Acta Crystallogr., Sect. B: Struct. Sci.*, 2007, **B63**, 735; https://doi.org/10.1107/S0108768107031758.
17 T.-T. Sha, Y.-A. Xiong, Q. Pan, X.-G. Chen, X.-J. Song, J. Yao, S.-R. Miao, Z.-Y. Jing, Z.-J. Feng, Y.-M. You and R.-G. Xiong, *Adv. Mater.*, 2019, **31**, 1901843; https://doi.org/10.1002/adma.201901843.
18 X.-G. Chen, X.-J. Song, Z.-X. Zhang, P.-F. Li, J.-Z. Ge, Y.-Y. Tang, J.-X. Gao, W.-Y. Zhang, D.-W. Fu, Y.-M. You and R.-G. Xiong, *J. Am. Chem. Soc.*, 2020, **142**, 1077; https://doi.org/10.1021/jacs.9b12368.
19 G. Huang, S. Rassel, J. Qu, S. Xu, C. Wang and D. Ban, *ACS Appl. Electron. Mater.*, 2021, **3**, 285; https://doi.org/10.1021/acsaelm.0c00852.
20 A. Lemmerer and D. G. Billing, *Dalton Trans.*, 2012, **41**, 1146; https://doi.org/10.1039/C0DT01805H.
21 P. Giannozzi, S. Baroni, N. Bonini, M. Calandra, R. Car, C. Cavazzoni, D. Ceresoli, G. L. Chiarotti, M. Cococcioni, I. Dabo, A. Dal Corso, S. de Gironcoli, S. Fabris, G. Fratesi, R. Gebauer, U. Gerstmann, C. Gougoussis, A. Kokalj, M. Lazzeri, L. Martin-Samos, N. Marzari, F. Mauri, R. Mazzarello, S. Paolini, A. Pasquarello, L. Paulatto, C. Sbraccia, S. Scandolo, G. Sclauzero, A. P. Seitsonen, A. Smogunov, P. Umari and R. M. Wentzcovitch, *J. Phys.: Condens. Matter*, 2009, **21**, 395502; https://doi.org/10.1088/0953-8984/21/39/395502.
22 K. Momma and F. Izumi, *J. Appl. Crystallogr.*, 2011, **44**, 1272; https://doi.org/10.1107/S0021889811038970.
23 E. I. Marchenko, S. A. Fateev, A. A. Ordinartsev, P. A. Ivlev, E. A. Goodilin and A. B. Tarasov, *Mendeleev Commun.*, 2022, **32**, 315; https://doi.org/10.1016/j.mencom.2022.05.007.
24 V. A. Blatov, A. P. Shevchenko and D. M. Proserpio, *Cryst. Growth Des.*, 2014, **14**, 3576; https://doi.org/10.1021/cg500498k.
25 P. R. Spackman, M. J. Turner, J. J. McKinnon, S. K. Wolff, D. J. Grimwood, D. Jayatilaka and M. A. Spackman, *J. Appl. Crystallogr.*, 2021, **54**, 1006; https://doi.org/10.1107/S1600576721002910.

Received: 14th May 2025; Com. 25/7823